## Appendix S1: Mathematical details on quasi-potential analysis

### Section 1: Stochastic Differential Equations

In example 1, we briefly described a stochastic differential equation model for lake eutrophication. In this section of the appendix, we provide background information about stochastic differential equations. A random variable $X$ is a variable whose value is subject to chance. When a specific outcome $X = x$ is observed, it is called a realization. A stochastic process $X(t)$ is a family of random variables indexed by the parameter $t$, which usually represents time. Time can be measured discretely or continuously; this latter case falls in the realm of stochastic differential equations. A realization, $X(t) = x(t)$, is obtained when the stochastic process is observed at each time $t$. Note that a realization $x(t)$ is a deterministic function of time.

A continuous-time stochastic process of particular importance is the Wiener process, also known as Brownian motion, and denoted by $W(t)$. This process can be visualized as the limit of a discrete time random walk, which changes by an amount $\Delta W$ per each time step $\Delta t$. Each increment $\Delta W$ is selected from a normal distribution with mean 0 and variance $\Delta t$. The Wiener process is the limit of this random walk as $\Delta t \to 0$. It turns out that the Wiener process is completely characterized by three properties:

1. $W(0) = 0$
2. $W(t)$ is almost surely continuous everywhere. This means that, with 100% probability, a realization will be continuous (aside from possibly a few bad points, which have measure zero).
3. If $0 \leq s_1 < t_1 \leq s_2 < t_2$, then $W(t_1) - W(s_1)$ is normally distributed with mean zero and variance $t_1 - s_1$, $W(t_2) - W(s_2)$ is normally distributed with mean zero and variance $t_2 - s_2$, and $W(t_1) - W(s_1)$ and $W(t_2) - W(s_2)$ are independent.

The Reimann-Stieljes integrals of elementary calculus are defined as the limits of finite sums. Integration with respect to a Wiener process can be defined in a similar way. The Itô

integral of the function $h$ of a stochastic process $X(t)$ over the interval $[0, T]$ is defined as

$$\int_0^T h(X(t))\, dW = \lim_{n\to\infty} \sum_{i=0}^{n-1} h(X(t_i))\, (W(t_{i+1}) - W(t_i)), \tag{S1}$$

where $\{[t_i, t_{i+1})\}_{i=0}^n$ is a partition of $[0, T]$. Note that this integral is a stochastic process itself; each realization of $X$ and $W$ leads to a different realization of the integral. In the Itô integral, $h(X(t))$ is evaluated at the left end points of the intervals of the partition. If a trapezoidal rule is used instead, then the result is the Stratonovich integral. In this paper, we use the Itô integral, because of the way it discriminates between the past and the future. A process $X(t)$ is called "non-anticipating" if its value at $t$ is independent of values of $W(s)$, for $s > t$. If $X(t)$ is non-anticipating, then the Itô integral defined above is, too. The Stratonovich integral is not, because calculating the integral at time $s$, $t_i \leq s < t_{i+1}$ requires knowledge of $X(t_{i+1})$. Basically, the Itô integral cannot "see into the future", while the Stratonovich integral can.

Having defined integration with respect to a Wiener process, we can now define a stochastic differential equation. Consider a deterministic autonomous differential equation,

$$\frac{dx}{dt} = f(x). \tag{S2}$$

In a small time period $\Delta t$, the variable $x$ changes by an amount of approximately $\Delta x = f(x)\, \Delta t$. Now suppose that the variable $x(t)$ is subject to random disturbances, and hence is a stochastic process $X(t)$. To approximate the value of this stochastic process at time $T$, we discretize time into $m$ small intervals, each of length $\Delta t$. Let $X_i = X\,(i\Delta t)$, and $\Delta X_i = X_{i+1} - X_i$. During a time period of length $\Delta t$, there are probably many small perturbations that affect $X$; if they have finite variance, then by the central limit theorem, adding these small perturbations up yields a normally distributed random variable. We will assume that this accumulated perturbation over a time period of length $\Delta t$ has mean 0 and variance $\sigma^2 \Delta t$ (the linear relationship with $\Delta t$ is required in order for $X(T)$ to have finite, non-zero variance in the continuous time limit). Therefore, the change in the stochastic

process over a time interval of length $\Delta t$ can be written as

$$\Delta X_i = f(X_i)\Delta t + \sigma \Delta W_i, \tag{S3}$$

where $\Delta W_i$ is normally distributed with mean 0 and variance $\Delta t$. Adding up the changes in the process over the time interval $[0, T]$ yields

$$X(T) = X(0) + \sum_{i=1}^{m} f(X_i)\Delta t + \sigma \sum_{i=1}^{m} \Delta W_i, \tag{S4}$$

which suggests an integral equation for the continuous time limit,

$$X(T) = X(0) + \int_0^T f(X)dt + \sigma \int_0^T dW. \tag{S5}$$

If the intensity of perturbations depend on the value of $X$, then equation (S.5) can be generalized to

$$X(T) = X(0) + \int_0^T f(X)dt + \sigma \int_0^T g\left(X\right) dW \tag{S6}$$

The integrals in equation (S6) make the notation cumbersome. In light of this, a modified notation is used. The stochastic differential equation

$$dX = f(X)\, dt + \sigma\, g(X)\, dW \tag{S7}$$

formally means that $X(t)$ is a solution to equation (S7). Note that $\frac{dW}{dt}$ does not exist, because the sample paths of $W\left(t\right)$ are almost surely nowhere differentiable. This is why the notation in equation (S7) is used; it reminds us that $X(t)$ is defined by the integral equation (S6).

**Section S2: Freidlin-Wentzell quasi-potential**

In this section, we provide a more formal definition of the Freidlin-Wentzell quasi-potential. Consider a system of stochastic differential equations

$$d\mathbf{X} = f(\mathbf{X})\, dt + \sigma\, g(\mathbf{X})\, d\mathbf{W}, \tag{S8}$$

where $\mathbf{X} = (X_1, \ldots, X_n)$ is a vector of state variables, $\mathbf{W} = (W_1, \ldots, W_m)$ is a vector of $m$ independent Wiener processes. Vectors in this paper should be interpreted as column vectors. The lower-case notation $\mathbf{x} = (x_1, \ldots, x_n)$ is used to indicate a point (as opposed to a stochastic process). $f$ is a vector field that is the deterministic skeleton of the system. $g(\mathbf{x})$ is a matrix that determines how the different noise sources affect the state variables, and $\sigma$ is the noise intensity. For simplicity, we will focus on the case where $m = n$ and $g(\mathbf{x})$ is the identity matrix, which represents constant-intensity isotropic noise, affecting each state variable with equal intensity. Under these assumptions, equation (S8) can be written as

$$d\mathbf{X} = f(\mathbf{X})\, dt + \sigma\, d\mathbf{W}. \tag{S9}$$

In Section S6, we will return to the general case (S8), but constant, isotropic noise provides a useful starting point. If there exists a function $U(\mathbf{x})$ such that $f = -\nabla U$, then the differential equations are called a gradient system, and the function $U$ is called a potential function. Like one-dimensional systems, a multi-dimensional gradient system can be viewed with the ball-in-cup framework. For $n = 2$, the relevant metaphor is a ball rolling on a two-dimensional surface specified by the function $U(\mathbf{x})$. For $n \geq 3$, the situation is difficult to visualize, but the same general intuitive aspects hold. The steady-state probability distribution of higher-dimensional gradient systems is related to the potential $U$ in the same way as in (6), except $\mathbf{x}$ replaces $x$ and $Z$ is obtained from an
$n$-dimensional integral. Expressions for the mean first passage time between stable equilibria separated by a saddle are similar to the one-dimensional case as well.

Unfortunately, gradient systems are a very special situation. In most cases of (S9), there will not exist a function $U$ satisfying $f = -\nabla U$. For these non-gradient systems, we cannot use a potential function to quantify stability, as we did in example 1. In what follows, we develop an approach that is conceptually analogous but applicable to non-gradient systems.

In the following, we will use the concept of logarithmic equivalence, denoted by $\asymp$. We

write $f(x) \asymp e^{\kappa h(x)}$ if

$$\lim_{\kappa \to \infty} \kappa^{-1} \ln(f(x)) = h(x). \tag{S10}$$

The Freidlin-Wentzell approach is to obtain a large deviation principle for trajectories $x(t)$ of (S9). In this context, a large deviation principle is an asymptotic rule that determines how likely it is for realizations of (S9) to depart from a given path. To make this concrete, let $\mathbf{a}$ be an asymptotically stable equilibrium of $\mathbf{f}$ in (S9). Let $\mathbf{b} \in \mathbb{R}^n$ and $T > 0$. Let $\Theta_T$ be the set of all absolutely continuous paths $\theta : [0, T] \to \mathbb{R}^n$ such that $\theta(0) = \mathbf{a}$ and $\theta(T) = \mathbf{b}$. We will study the probability that a realization $\mathbf{x}_\sigma(t)$ of (S9) with noise intensity $\sigma$ and with $\mathbf{x}_\sigma(0) = \mathbf{a}$ and $\mathbf{x}_\sigma(T) = \mathbf{b}$ stays close to $\theta \in \Theta_T$. A large deviation principle declares that there exists a $\delta_0 > 0$ such that, if $0 < \delta < \delta_0$, then

$$\Pr\left\{ \sup_{0 \le s \le T} |\mathbf{x}_\sigma(s) - \theta(s)| < \delta \right\} \asymp \exp\left( -\frac{S_T(\theta)}{\sigma^2} \right), \tag{S11}$$

where the logarithmic equivalence holds as $\sigma \to 0$. The functional $S_T : \Theta_T \to [0, \infty)$ is called the action, and it is defined by

$$S_T(\theta) = \frac{1}{2} \int_0^T \left| f(\theta(t)) - \dot{\theta}(t) \right|^2 dt. \tag{S12}$$

Note that $S_T$ measures how much $\dot{\theta}$ deviates from the vector field $f$. If $S_T(\theta) = 0$, then $\theta$ is a trajectory of the deterministic system, $\frac{dx}{dt} = f(x)$. The action $S_T$ is related to the probability distribution of $\mathbf{X}$ by

$$\lim_{\sigma \to 0} \sigma^2 \ln\left( \Pr\left\{ \mathbf{X}(T) \in \Omega | \mathbf{X}(0) = \mathbf{a} \right\} \right) = - \inf_{\theta \in \Theta_T} \left\{ S_T(\theta) | \theta(0) = \mathbf{a}, \theta(T) \in \Omega \right\}, \tag{S13}$$

where $\Omega$ is a domain in $\mathbb{R}^n$. For details on the technical assumptions behind this relationship, see Freidlin and Wentzell (2012). To get from $\mathbf{a}$ to $\mathbf{b}$ in a "likely" way, the action should be made as small as possible. This motivates the definition of the Freidlin-Wentzell quasi-potential (or simply quasi-potential), $\Phi_{\mathbf{a}} : \mathbb{R}^n \to [0, \infty)$,

$$\Phi_{\mathbf{a}}(\mathbf{b}) = \inf_{T > 0, \theta \in \Theta_T} \left\{ S_T(\theta) | \theta(0) = \mathbf{a}, \theta(T) = \mathbf{b} \right\}. \tag{S14}$$

Note that the infimum is taken over paths of all durations (that is, all times $T > 0$).

The quasi-potential is the value of the action for the minimum-action path (i.e., the most likely path) between $\mathbf{a}$ and $\mathbf{b}$. It is closely related to first passage times from domains of attraction. If $D$ is a region contained within the domain of attraction of $\mathbf{a}$, then the expected time until a trajectory exits $D$, $\tau_{\mathbf{a}}^{\partial D}$, is given by

$$\lim_{\sigma \to 0} \sigma^2 \ln(\tau_{\mathbf{a}}^{\partial D}) = \inf_{\mathbf{x} \in \partial D} \Phi_{\mathbf{a}}(\mathbf{x}). \tag{S15}$$

The quasi-potential need not be defined solely in terms of an isolated asymptotically stable equilibrium $\mathbf{a}$. Cameron (2012) generalized the quasi-potential, and defined it for compact sets. This generalization allows the quasi-potential to be determined for limit cycles (as demonstrated in example 3). A different approach to generalizing the quasi-potential to compact sets can be can be found in Freidlin and Wentzell (2012). Cameron's generalization requires considering the geometric action (Heymann and Vanden-Eijnden 2008*b*,*a*), which we will denote by $S^*$. Suppose that $\theta \in \Theta_T$, and $\psi(\nu)$ is a reparameterization of $\theta$ such that $\psi(0) = \theta(0)$ and $\psi(\nu_0) = \theta(T)$. Then the geometric action is

$$S^*(\psi) = \int_0^{\nu_0} |f(\psi(\nu))|\,|\dot{\psi}(\nu)| - f(\psi(\nu)) \cdot \dot{\psi}(\nu)\, d\nu. \tag{S16}$$

The value of $S^*$ is independent of the parameterization of $\psi$. If $A$ and $B$ are compact sets in $\mathbb{R}^n$, then the quasi-potential can be defined by

$$\Phi_A(B) = \inf \left\{ S^*(\psi) | \psi(0) \in A, \psi(\nu_0) \in B \right\}. \tag{S17}$$

**Section S3: A global quasi-potential**

In systems with multiple stable equilibria, it is desirable to obtain a global quasi-potential that describes how trajectories switch between states. In the preceding section, the quasi-potential was defined in terms of a stable equilibrium $\mathbf{a}$. Suppose now that there are two stable equilibria, $\mathbf{a}_1$ and $\mathbf{a}_2$, with corresponding domains of attraction $D_1$ and $D_2$. The action functionals can be used to obtain $\Phi_{\mathbf{a}_1}$ and $\Phi_{\mathbf{a}_2}$, but these quasi-potentials are of

limited utility outside of $D_1$ and $D_2$, respectively. The minimum action path from $\mathbf{a}_1$ to $\mathbf{a}_2$ will follow streamlines of the vector field once it enters $D_2$. This will result in no accumulated work; hence $\Phi_{\mathbf{a}_1}$ will be flat along streamlines in $D_2$. The quasi-potentials both describe dynamics well within their domains of attraction, but in order to create a complete surface in the spirit of a classical potential function, it is necessary to combine the two. This is easily accomplished if there is a single saddle point $\mathbf{s}$ that lies on the separatrix between $D_1$ and $D_2$. We find the constant

$$C = \Phi_{\mathbf{a}_1}(\mathbf{s}) - \Phi_{\mathbf{a}_2}(\mathbf{s}) \tag{S18}$$

so that $\Phi^*_{\mathbf{a}_2} = \Phi_{\mathbf{a}_2} + C$ agrees with $\Phi_{\mathbf{a}_1}$ at $\mathbf{s}$. Finally, we compute the global quasi-potential $\Phi$ as

$$\Phi(\mathbf{x}) = \min\left(\Phi_{\mathbf{a}_1}(\mathbf{x}), \Phi^*_{\mathbf{a}_2}(\mathbf{x})\right). \tag{S19}$$

More complicated cases can arise when domains of attraction are connected by more than one saddle (Freidlin and Wentzell 2012). For details about how to combine local quasi-potentials into a global quasi-potential in these more complicated cases, see Freidlin and Wentzell (2012), Moore et al. (Submitted), and Roy and Nauman (1995).

**Section S4: Small noise expansion of V**

This section describes the relationship between $V$ and $V_0$, and shows the derivation of the Hamilton-Jacobi equation for $V_0$. The Fokker-Planck equation associated with the two-dimensional version of (A.9) is (10). Under relatively mild conditions on the function $f$ (for details, see Freidlin and Wentzell 2012), there will exist a steady-state probability distribution

$$p_s(\mathbf{x}) = \lim_{t\to\infty} p(\mathbf{x}, t). \tag{S20}$$

Steady-state distributions can often be approximated by very long-time realizations. Determining when such an approximation holds is the subject of ergodic theory (see Arnold 2010). Approximations to steady-state distributions for the consumer-resource in

example 2 (i.e., the system (8)) are shown in Figure S1. Each panel corresponds to a different noise intensity, $\sigma$. Qualitatively, Figure S1 confirms that trajectories spend more time near $\mathbf{e}_A$ than $\mathbf{e}_B$, and hence a sensible stability metric should classify $\mathbf{e}_A$ as more stable than $\mathbf{e}_B$. However, it also clearly shows that the steady-state distribution depends on the noise level; each choice of $\sigma$ yields a different distribution. If one is interested in the general properties of the system, and not just the steady-state distribution for a specific noise intensity, then steady-states distributions are of limited utility.

The "effective potential" (not to be confused with the potential or quasi-potential) is defined as

$$V(\mathbf{x}) = -\frac{\sigma^2}{2} \ln p_s(\mathbf{x}) + C, \tag{S21}$$

where $C$ is a constant. The effective potential's relationship with the steady-state distribution makes it a helpful tool. The peaks of the steady-state distribution correspond to valleys of the effective potential, and vice versa. There are two reasons why we do not adopt the effective potential as a stability metric in this paper. First, the effective potential depends on $\sigma$, and hence suffers from the same issue as the steady-state distribution. In the ball-in-cup metaphor, the noise intensity $\sigma$ determines the perturbations of the ball as it rolls, rather than determining the shape of the landscape. Second, the effective potential is not a Lyapunov function for the deterministic system, so a trajectory of a system with zero noise does not necessarily move downhill. Finally, a decomposition based on the gradient of $V$is not orthogonal. Despite these shortcomings, the effective potential is closely related to the quasi-potential. Solving (S21) for $p_s(\mathbf{x})$ yields

$$p_s(\mathbf{x}) = e^{\frac{2C}{\sigma^2}} e^{-\frac{2V(\mathbf{x})}{\sigma^2}}. \tag{S22}$$

Substituting this into the Fokker-Planck equation yields

$$|\nabla V|^2 + f_1 \frac{\partial V}{\partial x_1} + f_2 \frac{\partial V}{\partial x_2} - \frac{\sigma^2}{2} \left( \nabla^2 V + \frac{\partial f_1}{\partial x_1} + \frac{\partial f_2}{\partial x_2} \right) = 0. \tag{S23}$$

To simplify this equation, we consider how the system behaves for small noise values, and

expand $V$ in terms of the small parameter $\epsilon = \frac{\sigma^2}{2}$. This yields

$$V(\mathbf{x}) = \sum_{i=0}^{\infty} V_i(\mathbf{x})\epsilon^i, \tag{S24}$$

where $V_i$ is the coefficient function associated with order $\epsilon^i$. Inserting this into (S23) and retaining lowest-order terms, we obtain the Hamilton-Jacobi equation for $V_0$,

$$|\nabla V_0|^2 + f_1 \frac{\partial V_0}{\partial x_1} + f_2 \frac{\partial V_0}{\partial x_2} = 0. \tag{S25}$$

**Section S5: Hamilton-Jacobi equation for the quasi-potential**

By deriving the Hamilton-Jacobi equation for the quasi-potential, we can verify the relationship $\Phi = 2V_0$. This relationship is crucial. We described key properties about $V_0$ concerning the effective potential, the steady-state probability distribution, the Lyapunov property, and the orthogonality of the decomposition $f = -\nabla V + Q$; in Section S2, we described properties of $\Phi$. The relationship $\Phi = 2\,V_0$ shows that these functions share those properties; they only differ by multiplication of a scalar.

Bellman's Principle from optimal control theory can be used to derive the Hamilton-Jacobi equation for $\Phi$. We sketch the proof from Cameron (2012). The calculation of $\Phi_A(\mathbf{x})$, the value of the quasi-potential starting at a compact set $A$ and going to a point $\mathbf{x}$, can be viewed as an optimal control problem. We seek to minimize the value function $\Phi_A(\mathbf{x})$ by choosing an optimal path $\psi(\nu)$. This path is controlled by the velocity vector $\dot{\psi}(\nu)$. We are free to choose the parameterization of $\psi(\nu)$, so we select one where the velocity vector has unit magnitude at every point. The optimal control problem amounts to determining the tangent direction $\dot{\psi}(\nu)$ for each $\nu$, so that the resulting path minimizes the action. Bellman's Principle essentially turns this problem into a recursive equation. Heuristically, one can imagine the last segment of an optimal path $\psi(\nu)$ from $\psi(0) \in A$ to $\psi(K) = \mathbf{x}$. This last segment is specified by the parameter values $\nu \in [K - \delta, K]$. Clearly this optimal path will be optimal over the interval $[K - \delta, K]$. Therefore, if one knows the optimal path up to parameter value $K - \delta$, one knows the remainder of the path as well.

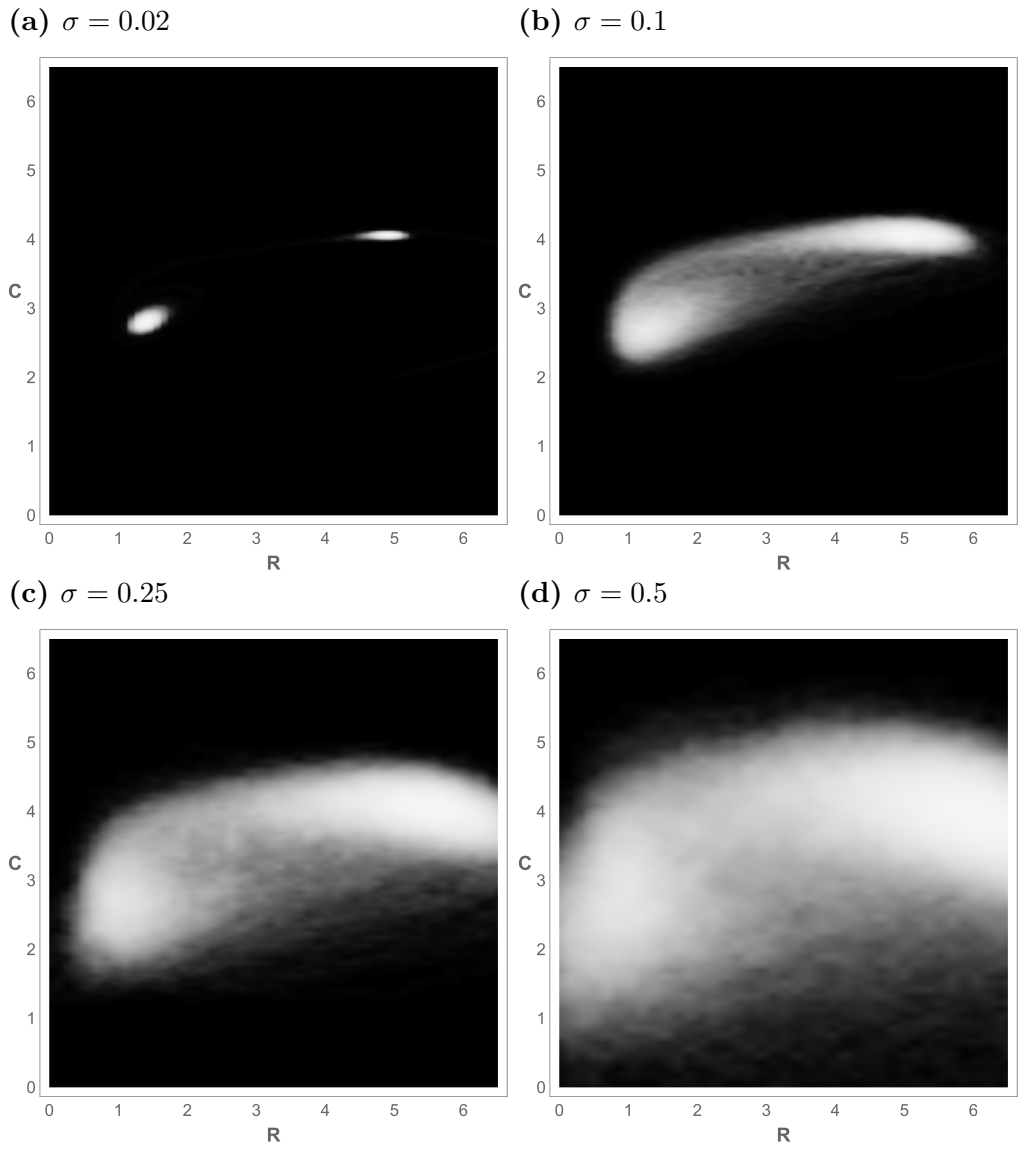


**Figure S1.** Approximations to the steady-state probability density of equations (8), obtained from a long-time ($t = 25000$) simulation, with four different noise intensities. Integration was performed with the Euler-Maruyama method and $\Delta t = 0.025$. Variables are scaled, so the units are dimensionless. The horizontal axis is resource population density and the vertical axis is consumer population density. White corresponds to high probability density. The information conveyed in each plot depends on the noise intensity (see Section S4).

Mathematically, this principle takes the form

$$\Phi_A(\mathbf{x}) = \inf_{\dot{\psi}\in\mathbb{S}^{n-1}} \left\{ \int_{K-\delta}^{K} |f(\psi(\nu))| - f(\psi(\nu)) \cdot \dot{\psi}(\nu)\, d\nu + \Phi_A\left(\psi(K-\delta)\right) \right\}. \tag{S26}$$

A small $\delta$ expansion yields

$$\Phi_A(\mathbf{x}) = \inf_{\dot{\psi}\in\mathbb{S}^{n-1}} \left\{ (|f(\mathbf{x})| - f(\mathbf{x})\cdot\dot{\psi})\delta + \Phi_A(\mathbf{x}) - \nabla\Phi_A(\mathbf{x})\cdot\dot{\psi}\,\delta \right\}. \tag{S27}$$

Solving this equation is equivalent to solving

$$\inf_{\dot{\psi}\in\mathbb{S}^{n-1}} \left\{ |f(\mathbf{x})| - f(\mathbf{x})\cdot\dot{\psi} - \nabla\Phi_A(\mathbf{x})\cdot\dot{\psi} \right\} = 0. \tag{S28}$$

Using the Cauchy-Schwarz inequality, one finds that the infimum of the left-hand side of (S28) occurs when

$$\dot{\psi} = \frac{f(\mathbf{x}) + \nabla\Phi_A(\mathbf{x})}{|f(\mathbf{x})|}. \tag{S29}$$

Substituting this into (S28) yields

$$|\nabla\Phi_A|^2 + 2\,\nabla\Phi_A\cdot f = 0. \tag{S30}$$

Comparing this to (12), we can see that, if solutions exist, they have the relationship $\Phi_A = 2\,V_0$. Classical solutions do not always exist for the Hamilton-Jacobi equation, so it is often necessary to consider a class of weak solutions called "viscosity solutions" (Sethian and Vladimirsky 2001, Crandall and Lions 1983, Crandall et al. 1984). When a classical solution does exist, it coincides with the viscosity solution.

**Section S6: Other noise structures**

This paper focuses on the case $g(\mathbf{x}) = I$ in equation (S8), where $I$ is the identity matrix. The quasi-potential can be calculated for more general cases. Such a generalization requires a modification in the definition of the action:

$$S_T(\theta) = \frac{1}{2}\int_0^T \sum_{i,j} q_{i,j}(\theta(t)) \left( f_i(\theta(t)) - \dot{\theta}_i(t) \right) \left( f_j(\theta(t)) - \dot{\theta}_j(t) \right) dt. \tag{S31}$$

where $q(x) = \left(g(x)g^T(x)\right)^{-1}$. The large deviation relationships, (S11) and (S13), are still valid. The Hamilton-Jacobi equation for (S8) is

$$\sum_{i,j} q_{i,j} \frac{\partial \Phi}{\partial x_i} \frac{\partial \Phi}{\partial x_j} + 2\,\nabla\Phi \cdot f = 0. \tag{S32}$$

Alternatively, one can find a transform of (S8) that turns the system into the form (S9), compute the quasi-potential in these new coordinates, and then back-transform to the original coordinates. For the system

$$\begin{aligned} dX_1 &= f_1(X_1,\, X_2)\, dt + \sigma\, g_1\, dW_1 \\ dX_2 &= f_2(X_1,\, X_2)\, dt + \sigma\, g_2\, dW_2, \end{aligned} \tag{S33}$$

where $g_1$ and $g_2$ are constants, the appropriate transform is $\tilde{X}_1 = g_1^{-1}\, X_1$, $\tilde{X}_2 = g_2^{-1}\, X_2$. For the system

$$\begin{aligned} dX_1 &= f_1(X_1,\, X_2)\, dt + \sigma\, g_1\, X_1\, dW_1 \\ dX_2 &= f_2(X_1,\, X_2)\; dt + \sigma\; g_2\, X_2\, dW_2, \end{aligned} \tag{S34}$$

the appropriate transform is $\tilde{X}_1 = g_1^{-1} \ln(X_1)$, $\tilde{X}_2 = g_2^{-1} \ln(X_2)$.

**Section S7: Curvature**

The concept of curvature is more nuanced for surfaces than it is for curves. The principal curvatures of the surface specified by $V_0$ at $\mathbf{e_0}$ are the largest and smallest curvatures of the one-dimensional normal sections at $\mathbf{e_0}$. A normal section is obtained by intersecting a plane containing the normal vector of the surface $V_0$ at $\mathbf{e_0}$ with $V_0$. The principal curvatures correspond to the eigenvalues of the Hessian matrix of $V_0$. In the gradient case, $f = -\nabla V_0$, so the Hessian matrix of $V_0$ is simply the negative of the Jacobian matrix of $f$. In other words, the principal curvatures of the surface $V_0$ are the eigenvalues obtained from the linear stability analysis (except with the sign changed).

**Section S8: Mean first passage time asymptotics**

Steady-state probability densities and mean first passage times can be determined from the quasi-potential, but only in the small-noise limit. These quantities are often expressed

in terms of logarithmic equivalence as $\sigma \to 0$. Accurate calculation involves not just the exponential part of the relationship, but also the prefactor. For a gradient system with potential $U$, the mean first passage time $\tau$ to transition from a stable equilibrium $\mathbf{x}$ to a saddle $\mathbf{z}$ is (Bovier et al. 2004):

$$\tau = \frac{2\,\pi}{|\lambda_1\,(\mathbf{z})|}\sqrt{\frac{|\det \nabla^2 U(\mathbf{z})|}{\det \nabla^2 U(\mathbf{x})}}\exp\left(\frac{2\,(U(\mathbf{z}) - U(\mathbf{x}))}{\sigma^2}\right)(1 + \mathcal{O}\,(\sigma\,|\log\,(\sigma)|)) \tag{S35}$$

$\nabla^2 U(\mathbf{z})$ is the Hessian of the potential at $\mathbf{z}$, and $\nabla^2 U(\mathbf{x})$ is the Hessian of the potential at $\mathbf{x}$. $\lambda_1(\mathbf{z})$ is the negative eigenvalue of the Hessian at the saddle. Bouchet and Reygner (2015) obtained a similar expression has for a non-gradient system with quasi-potential $V$. Their estimate for $\tau$ is

$$\tau = \frac{2\,\pi}{|\lambda_1\,(\mathbf{z})|}\sqrt{\frac{|\det \nabla^2 V(\mathbf{z})|}{\det \nabla^2 V(\mathbf{x})}}\exp\left(\frac{2\,(V(\mathbf{z}) - V(\mathbf{x}))}{\sigma^2}\right)\exp\left(\int_{-\infty}^{\infty} F(\rho(t))\,dt\right). \tag{S36}$$

$\lambda_1(\mathbf{z})$ is the unstable eigenvalue of the full deterministic skeleton (not just the quasi-potential) at the saddle. $\rho(t)$ is the least action path from $\mathbf{x}$ to $\mathbf{z}$:

$$\rho'(t) = \nabla V\,(\rho(t)) + Q\,(\rho(t)) \tag{S37}$$

$F$ is the divergence of the circulatory component, $F(\mathbf{x}) = \nabla \cdot Q(\mathbf{x})$.

For example 2, we can examine how the mean first passage time estimates from the quasi-potential correspond to simulation results (figure S2). For this example, numerical integration along the least action path suggests that $\int_{-\infty}^{\infty} F(\rho(t))\,dt \approx 0$, so we drop this term in the approximation. Note that the quasi-potential approximations closely match the means of the simulated first passage times. Of course, there will always be outliers, and these can be seen in the tails of the distributions of simulated first passage times in figure S2.

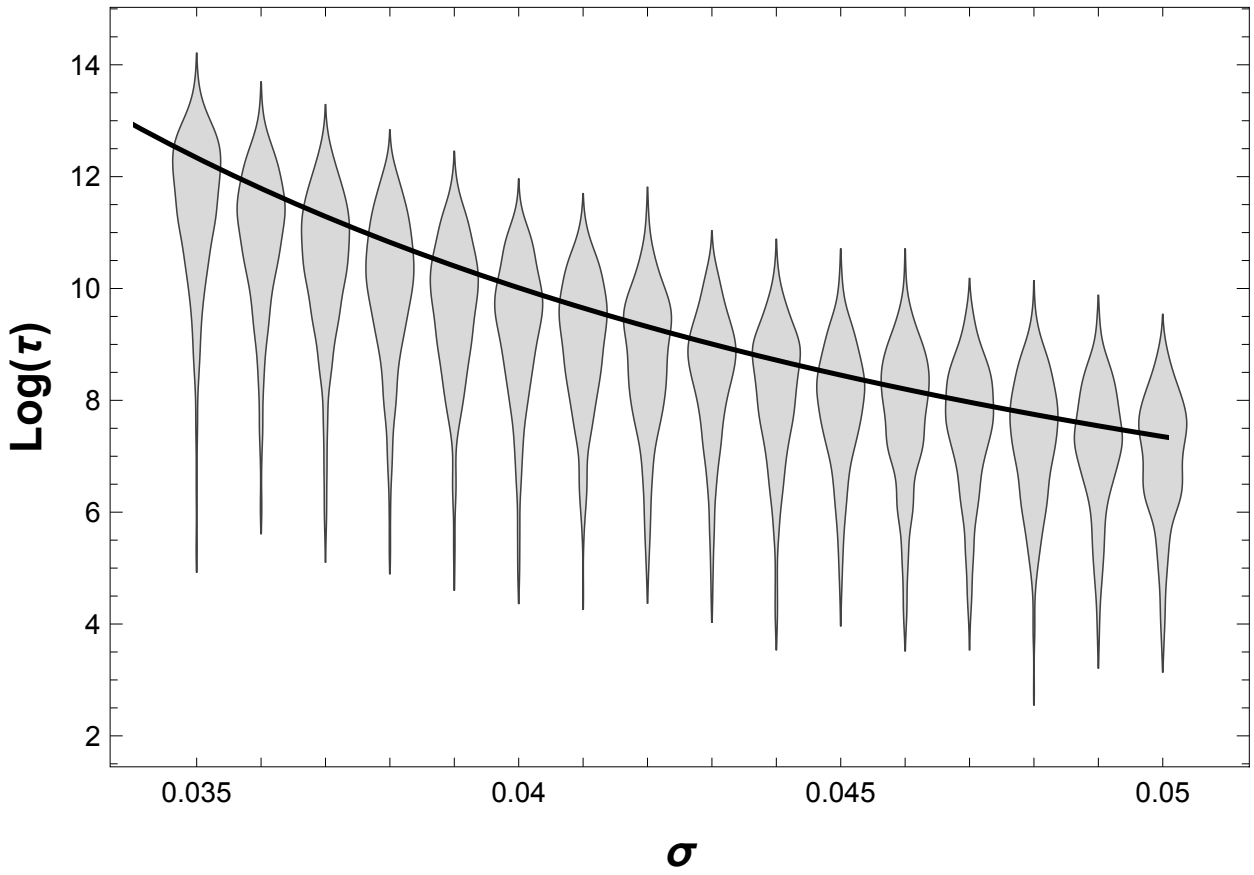


**Figure S2.** Simulation results for first passage times in example 2. The initial point is $\mathbf{e_A}$, and the time step is 0.05. 500 realizations were generated at each noise level. The width of each gray shape corresponds to the frequency with which each first passage time was observed. The black line is the small-noise approximation of the mean first passage time from the formula in appendix S8. Note that the small-noise approximation matches the means of the distributions well. At all noise levels, the simulations included outliers that escaped from the basin of attraction much faster than the small-noise prediction.

## Section S9: Further example

In the following, we examine a bistable model that illustrates the different ways that the stability metrics described in this paper can classify stable states. The model is

$$\begin{aligned} dX &= f_1(X,Y)\,dt + \sigma\,dW_1 \\ dY &= f_2(X,Y)\,dt + \sigma\,dW_1. \end{aligned} \tag{S38}$$

The deterministic skeleton is given by

$$f_1(x,y) = -2\,a\,b_1\,x\,\exp\left(-\left(b_1\,x^2 + b_2\,y^2\right)\right) - 2\,d_1\,\left(x-c\right)\exp\left(\left(d_1\,\left(x-c\right)^2 + d_2\,\left(y-c\right)^2\right)\right)$$

$$f_2(x,y) = -2\,a\,b_2\,x\,\exp\left(-\left(b_1\,x^2 + b_2\,y^2\right)\right) - 2\,d_2\,\left(y-c\right)\exp\left(\left(d_1\,\left(x-c\right)^2 + d_2\,\left(y-c\right)^2\right)\right)$$

. (S39)

This model does not represent any particular ecological process and was instead chosen for its ability to illustrate the range of relationships that are possible between the stability metrics we discuss. This is a gradient system, with potential function

$$U(x,y) = 1 - a\,\exp\left(-\left(b_1\,x^2 + b_2\,y^2\right)\right) - \exp\left(-\left(d_1\,\left(x-c\right)^2 + d_2\,\left(y-c\right)^2\right)\right). \quad \text{(S40)}$$

For all of the parameter values we consider, the system will have two stable states, $\mathbf{e}_1$ and $\mathbf{e}_2$, separated by a saddle $\mathbf{e}_s$. This example will show that each equilibria can be classified as more stable by any combination of the stability metrics. Without loss of generality, the stable-state with larger $x$ -value, $\mathbf{e}_2$, will be more stable according to metric 3 (the basin depth metric).

In case 1, the parameter values are $a = 0.9$, $b_1 = 1$, $b_2 = 1$, $c = 1.2$, $d_1 = 1.2$, $d_2 = 1.2$. $\mathbf{e}_2$ is more stable by all three metrics (figure S3).

$$\begin{aligned}
&\text{Metric 1: } \mathrm{Re}\left(\lambda\left(\mathbf{e}_1\right)\right) = -1.16769, \quad \mathrm{Re}\left(\lambda\left(\mathbf{e}_2\right)\right) = -1.75728 \\
&\text{Metric 2: } \left\|\mathbf{e}_1 - \mathbf{e}_s\right\| = 0.643635, \quad \left\|\mathbf{e}_2 - \mathbf{e}_s\right\| = 0.859567 \\
&\text{Metric 3: } U\left(\mathbf{e}_s\right) - U\left(\mathbf{e}_1\right) = 0.0842552, \quad U\left(\mathbf{e}_s\right) - U\left(\mathbf{e}_2\right) = 0.204706
\end{aligned} \quad \text{(S41)}$$

In case 2, the parameter values are $a = 0.9$, $b_1 = 2$, $b_2 = 2$, $c = 1.8$, $d_1 = 0.8$, $d_2 = 0.8$. $\mathbf{e}_2$ is more stable by metric 3 (depth) and metric 2 (basin width) but not metric 1 (linear

stability) (figure S4).

$$\begin{aligned} \text{Metric 1: } \mathrm{Re}\left(\lambda\left(\mathbf{e}_1\right)\right) &= -3.51331, \quad \mathrm{Re}\left(\lambda\left(\mathbf{e}_2\right)\right) = -1.59979 \\ \text{Metric 2: } \left\|\mathbf{e}_1 - \mathbf{e}_s\right\| &= 1.05186, \quad \left\|\mathbf{e}_2 - \mathbf{e}_s\right\| = 1.48722 \\ \text{Metric 3: } U\left(\mathbf{e}_s\right) - U\left(\mathbf{e}_1\right) &= 0.639468, \quad U\left(\mathbf{e}_s\right) - U\left(\mathbf{e}_2\right) = 0.73379 \end{aligned} \tag{S42}$$

In case 3, parameter values are $a = 0.9$, $b_1 = 1$, $b_2 = 1$, $c = 2.5$, $d_1 = 1.2$, $d_2 = 1.2$. $\mathbf{e}_2$ is more stable by metric 3 (depth) and metric 1 (linear stability), but not metric 2 (basin width) (figure S5).

$$\begin{aligned} \text{Metric 1: } \mathrm{Re}\left(\lambda\left(\mathbf{e}_1\right)\right) &= -1.79998, \quad \mathrm{Re}\left(\lambda\left(\mathbf{e}_2\right)\right) = -2.39984 \\ \text{Metric 2: } \left\|\mathbf{e}_1 - \mathbf{e}_s\right\| &= 1.81859, \quad \left\|\mathbf{e}_2 - \mathbf{e}_s\right\| = 1.71693 \\ \text{Metric 3: } U\left(\mathbf{e}_s\right) - U\left(\mathbf{e}_1\right) &= 0.837959, \quad U\left(\mathbf{e}_s\right) - U\left(\mathbf{e}_2\right) = 0.937962 \end{aligned} \tag{S43}$$

In case 4, the parameter values are $a = 0.9$, $b_1 = 0.9$, $b_2 = 0.9$, $c = 2.37$, $d_1 = 0.78$, $d_2 = 1.46$. $\mathbf{e}_2$ is more stable by metric 3 (depth), but not metric 1 (linear stability) or metric 2 (basin width) (figure S6).

$$\begin{aligned} \text{Metric 1: } \mathrm{Re}\left(\lambda\left(\mathbf{e}_1\right)\right) &= -1.61995, \quad \mathrm{Re}\left(\lambda\left(\mathbf{e}_2\right)\right) = -1.55978 \\ \text{Metric 2: } \left\|\mathbf{e}_1 - \mathbf{e}_s\right\| &= 1.80573, \quad \left\|\mathbf{e}_2 - \mathbf{e}_s\right\| = 1.77222 \\ \text{Metric 3: } U\left(\mathbf{e}_s\right) - U\left(\mathbf{e}_1\right) &= 0.81102, \quad U\left(\mathbf{e}_s\right) - U\left(\mathbf{e}_2\right) = 0.91103 \end{aligned} \tag{S44}$$

These four cases show that an equilibrium in a bistable system can be classified as "more stable" by any combination of the three metrics. Hence it is important to recognize that each metric conveys a different piece of information about stability.

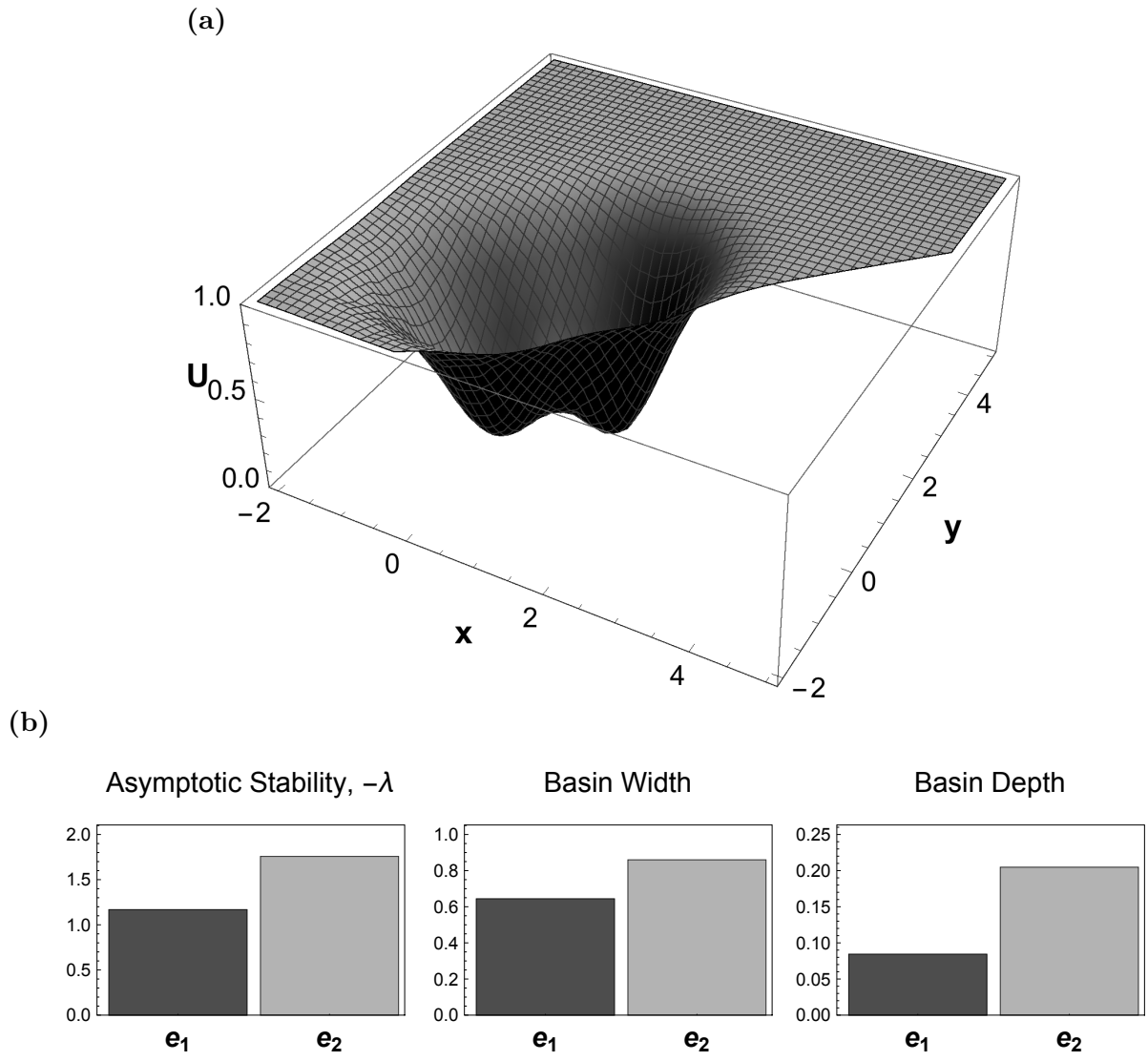


**Figure S3.** **(a)** The potential function for case 1 of the system in Section S9. **(b)** A comparison of three different metrics of stability for the system in case 1.

**(a)**

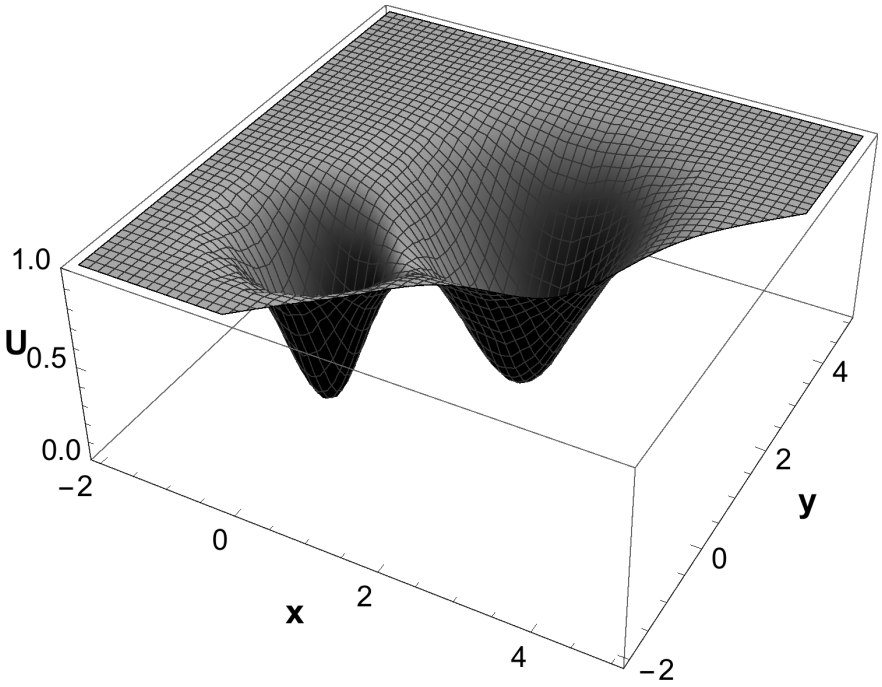


**(b)**

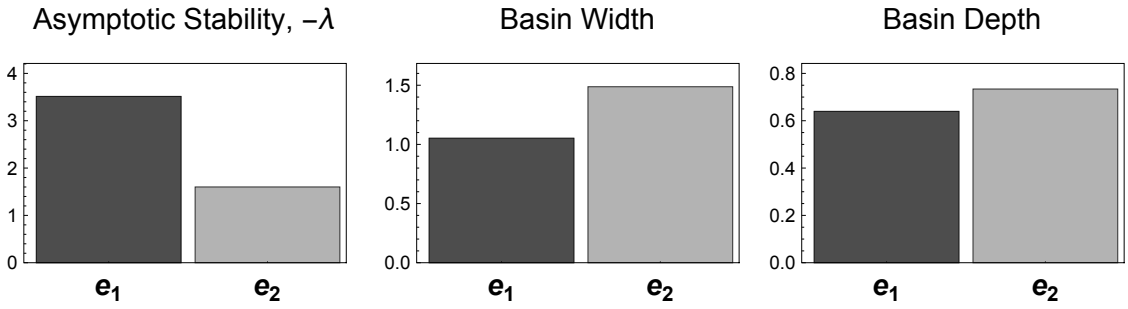


**Figure S4.** **(a)** The potential function for case 2 of the system in Section S9. **(b)** A comparison of three different metrics of stability for the system in case 2.

**(a)**

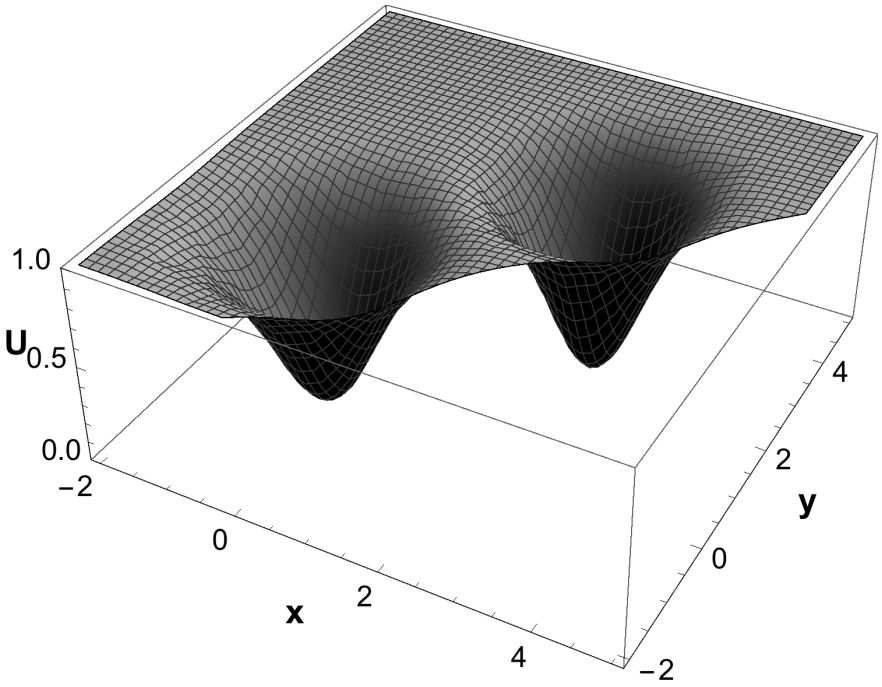


**(b)**

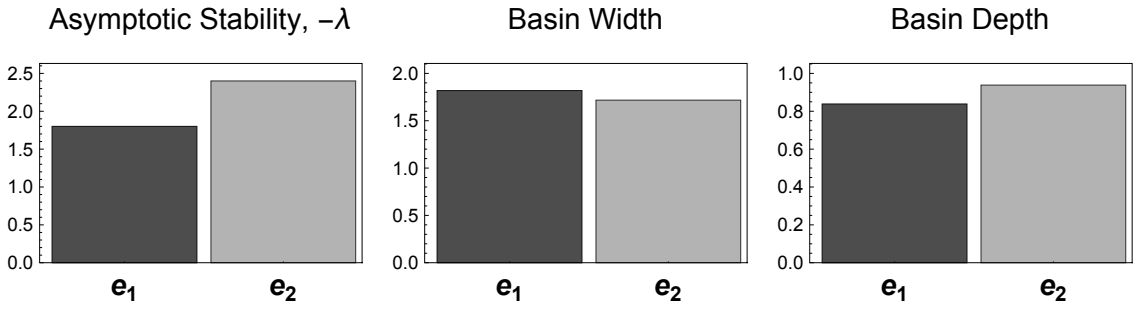


**Figure S5.** **(a)** The potential function for case 3 of the system in Section S9. **(b)** A comparison of three different metrics of stability for the system in case 3.

**(a)**

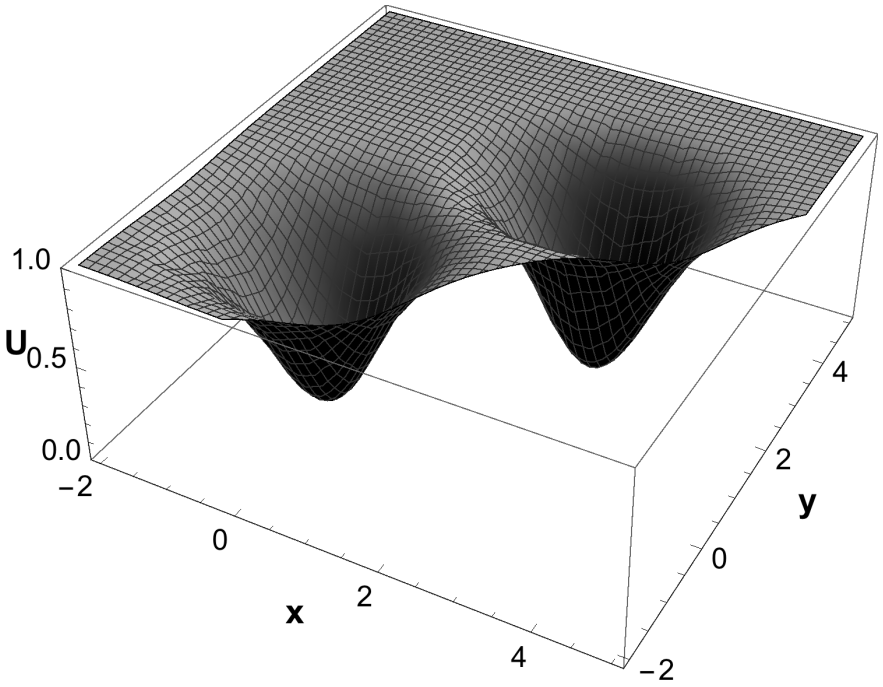


**(b)**

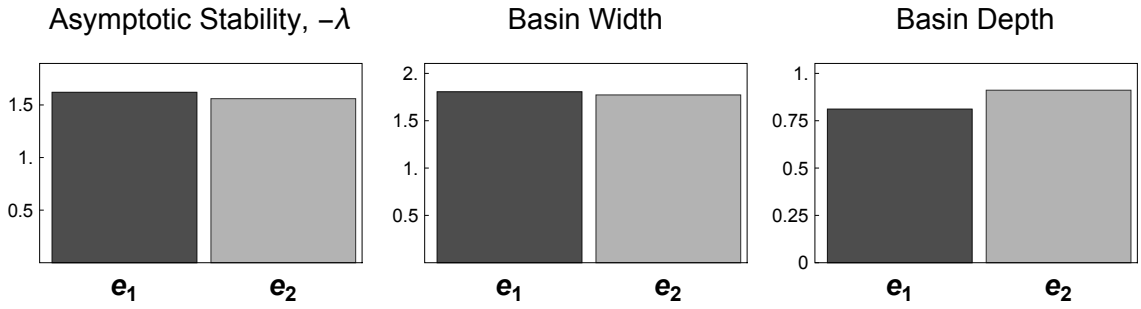


**Figure S6.** **(a)** The potential function for case 4 of the system in Section S9. **(b)** A comparison of three different metrics of stability for the system in case 4.

## References


Arnold, L. 2010. Random Dynamical Systems. Springer Monographs in Mathematics. Springer Berlin Heidelberg.

Bouchet, F., and J. Reygner. 2015. Generalisation of the Eyring-Kramers transition rate formula to irreversible diffusion processes. arXiv.org .

Bovier, A., M. Eckhoff, V. Gayrard, and M. Klein. 2004. Metastability in Reversible Diffusion Processes: Sharp Asymptotics for Capacities and Exit Times. J. Europ. Math. Soc. 6:399–422.

Cameron, M. K. 2012. Finding the quasipotential for nongradient SDEs. Physica D 241:1532–1550.

Crandall, M. G., L. C. Evans, and P.-L. Lions. 1984. Some properties of viscosity solutions of Hamilton-Jacobi equations. Transactions of the American Mathematical Society 282:487–502.

Crandall, M. G., and P.-L. Lions. 1983. Viscosity solutions of Hamilton-Jacobi equations. Transactions of the American Mathematical Society 277:1–42.

Freidlin, M. I., and A. D. Wentzell. 2012. Random perturbations of dynamical systems, vol. 260 of *Grundlehren der mathematischen Wissenschaften*. Springer.

Heymann, M., and E. Vanden-Eijnden. 2008*a*. The geometric minimum action method: A least action principle on the space of curves. Communications on pure and applied mathematics 61:1052–1117.

———. 2008*b*. Pathways of maximum likelihood for rare events in nonequilibrium systems: application to nucleation in the presence of shear. Physical Review Letters 100:140601.

Moore, C. M., C. R. Stieha, B. C. Nolting, M. K. Cameron, and K. C. Abbott. Submitted. QPot: An R package for stochastic differential equation quasi-potential analysis. The R Journal .

Roy, R., and E. Nauman. 1995. Noise-induced effects on a non-linear oscillator. Journal of Sound and Vibration 183:269–295.

Sethian, J. A., and A. Vladimirsky. 2001. Ordered upwind methods for static Hamilton–Jacobi equations. Proceedings of the National Academy of Sciences 98:11069–11074.